SPE/ISRM 47208

Understanding The Present day In-Situ State of Stress in the Cusiana Field - Colombia

P. A. Charlez Total Oil Marine, E. Bathellier CGG, C. Tan and O. Francois Altran-Technologies

This paper was prepared for presentation at the SPE/ISRM Eurock '98 held in Trondheim, Norway, 8–10 July 1998

Abstract

Compressional tectonics in the Eastern Cordillera foothills are investigated using a large strain, two-dimensional finite element method. The main purpose is to calculate the stress regimes within the Cusiana field and to compare the results with field data.

In the foothills, the NW-SE tectonic push is clearly confirmed by borehole breakouts. The present-day state of stress in the Cusiana field, is investigated through a footwall-hangingwall model with a detachment/ramp thrust fault. The tectonic push was simulated by applying horizontal displacement to the vertical boundary of the model. Simulations with both elastic and elastoplastic rheologies were performed.

To obtain a realistic horizontal stress gradient (in the range of 1.25 to 1.5 psi/ft) at depth, the stiffness of the hangingwall block has to be sufficiently low to accomodate the thrust geometry. With a perfectly sliding fault (zero friction), the tectonic push localizes the plastic deformation into a shear band which can be interpreted as the backthrust observed on the seismic section. Moreover, in the vicinity of the Cusiana thrust, the major principal stress rotates. This rotation is in good agreement with orientation found by core DSCA measurements.

Introduction

From the beginning of the 90's, large amounts of crude oil have been discovered in the Colombian foothills[1]. Due to active tectonics, the drilling problems encountered (extended cavings, large mud losses, stuck pipe problems, hard reaming while tripping) in the Cusiana/Cupiagua structure were unprecedented, some wells being side tracked several times before reaching the target[2]. Wellbore instability and mud losses being closely linked to in situ stresses, a better understanding of the present-day stress regime in the whole structure was of a strategic importance to improve drilling performances.

Several methods are available to measure stresses both in-situ (hydraulic fracturing[3], analysis of borehole breakouts[4]) or using core material (differential strain curve analysis[5], anelastic strain recovery[6]). In passive margins, stress state being quite homogeneous, data obtained from a borehole can possibly be used to design a neighbouring well. However, in very tectonic areas, given the high variabilty of the stress state (both vertically and horizontally) such extrapolation is not possible.

The alternative method is a comprehensive modelling of the whole structure using borehole and core data as guidelines and/or calibration points. Since the early work of Hafner[7] and Sanford[8], geomechanical models have been used to compute stress fields in geological structures. For instance, several finite element studies on stress regimes induced by subduction have been published during the last ten years [9,10,11,12,13,14] as well as stress computations in compressive sedimentary basins[15,16]. However, the numerical methods used did not simulate both displacements along faults and large strains. The goal of this paper is to compute the present-day stress regime in the Eastern Cordillera foothills where the Cusiana field is located. When possible the computed stresses (magnitude and/or orientation) will be compared with field data.

Regional geology of the Andean Cordilliera

The Colombian Andes are made of three Cordilleras set by alternance of extensive and compressive regimes [17,18]. Since the Middle Miocene, the Eastern Cordillera builds by shortening and tectonic inversion of mesozoic basins. Today, the compressive front continues to migrate towards the East.

From West to East, six tectonic regions can be identified according to their stress regimes (**Fig. 1**): forearc, western volcanic chain, altiplano, Cordillera, foothills and llanos.
The forearc is located along the Pacific ocean between the trench and the flanks of the volcanoes. It is characterized by a compressional stress drop and an extensional strain field[9].

The volcanic region bounds the forearc. The high temperatures required for volcanism are generated by frictional heating along the subduction megafault between the descending lithosphere and the overlying continent. Like the forearc, the altiplano located behind the volcanic chain is characterized by an extensional strain field. Unlike the forearc and the altiplano, the Cordillera and the foothills are characterized by a compressive stress regime. The shortening resulting from this compressional stress state is accommodated in the foothills by large thrust and strike-slip faults. These major discontinuities release the stresses in the llanos foreland basin, which is for this reason tectonically passive and undeformed.

The foothills of the Colombian Andean Cordillera - The Cusiana field

The Cusiana field is located in the central part of Colombia near Yopal (**Fig. 2**). The oil structure which is elongated parallel to the Eastern Cordillera (i. e. NE-SW) lies in the foothills. This tectonically active area is characterized by two major thrust faults: the Yopal fault and the Cusiana fault (**Fig. 3**). These two major discontinuities divide the structure into three blocks respectively called from NW to SE, Yopal, Cusiana and Llanos. In the considered cross section, a backthrust emerges at depth from the Cusiana fault and points towards the surface. The upper part of this backthrust is shifted upwards. This is a proof that the Yopal fault was activated after the Cusiana fault. The Yopal fault located on the west side of the block trends NE-SW and dips towards West. In the central part of the field, the Cusiana fault is pseudo-parallel to the Yopal fault. Let us observe the great structural complexity of Yopal and Cusiana blocks (which suggests large stress variabilities) comparing to the weakly deformed Llanos block.

The sedimentary cover contains three major formations overlying the reservoirs (ranging from 3400m to 5000m depending on location): the Guayabo (reddish soft clay), Leon (dark hardened shales) and finally Carbonera which is an alternance of sandstones and shales (nine different levels C1 to C9 - the even numbers are sandstones and the odd numbers are shales). The hydrocarbons being trapped in the Cusiana block, it is hence necessary to cross the Yopal thrust fault before reaching the reservoir.

The current state of stress in the Cusiana field is related to the force balance between Nazca, Caribbean, and South American plates. Inversion of shallow focal mechanisms shows that in the considered area the tectonic thrust trends roughly NW-SE and suggests that the maximum and the minimum principal stresses are horizontal while the intermediate stress is vertical. This hypothesis is confirmed below using borehole breakouts, core analysis and hydraulic fracturing stress measurements.

Evidence of a regional tectonics - Analysis of breakouts

Deep wells are rarely circular. This phenomenon, known as ovalisation is the result of a more or less intense deterioration of the mechanical properties of the material in the vicinity of the borehole. This deterioration often occurs in a preferential direction known as the direction of ovalisation. Uniformity of the ovalisation direction, both vertically (sometimes several hundreds of meters in a same well) and horizontally (over several dozen square km) quickly attracted the attention of geomechanicians but Bell and Gough[19] were the first to point out the role played by geostatic stresses on borehole ovalisation. In effect, it can easily be shown[20,21] that in an anisotropic stress field, the direction of ovalisation is parallel to the minor geostatic stress. Following this proposal, it is then possible to identify the direction of a tectonic thrust which should be perpendicular to the ovalisation direction.

Ovalisation of deep wells can be measured by using a dipmeter. Data produced by the dipmeter (minimum diameter, maximum diameter and azimuth) can only be interpreted in terms of tectonics after a rigorous selection of the really representative events. Before any detailed analysis, it is recommended to smooth the raw data to attenuate variations. Once the signal has been filtered, it is analysed by vertical and lithological sections. Three types of events can be identified at this stage (**Fig. 4**). If the well is not ovalised (calliper equal to the diameter of the bit), it is said to be *"in gauge"*. If the well is clearly ovalised in one direction, but remains more or less calibrated in the perpendicular direction, the term *"breakout"* is used. Finally, if it is ovalised in both directions, this is called a *"washout"*. The type of event will have a considerable impact on the estimated azimuth. For an in-gauged section or a washout, the cross-section being pseudo-circular the probe will be able to rotate freely around the wire line. Thus, the azimuth will have no physical meaning. However, in the case of a clearly marked breakout, one of the arms will block in the caving and the azimuth will then be representative of the ovalisation direction. All azimuth data resulting from washouts or in-gauge sections shall be systematically eliminated.

These phenomena are clearly illustrated on **Fig. 5** which gives a synthesis of all three events on the same cross-section, i.e., a breakout, an in-gauge section, a washout and finally a second breakout. Only the two breakouts will be considered in this latter case. The azimuth, stable in the *"breakout"* zones, is very disturbed in the in-gauge and the washout sections. The latter must be eliminated.

Caliper data of 7 vertical wells from dipmeter were treated and only 10% of the overall information was kept. 68 events were identified in the category of breakouts. The distribution of these events (the values given are the mean azimuths of the considered sections) is shown on **Fig. 6a**. We can clearly observe a very high density of events (about 80%)

concentrated between N30°E and N50°E. These results are confimed if the analysis is performed well by well (**Fig. 6b**). In the latter, UBI data were mixed with classical calliper data[2]. As previously suggested, breakout data clearly confirm that the actual regional compressive tectonic stress is NW-SE.

Stress magnitudes

Only few hydraulic fracturing measurements are available in the Cusiana field. As pointed out by Last and al[2], the minimal stress gradient estimated from two step rate tests performed in the reservoir is in the range of 0.65 psi/ft. This quite low value (a value generally accepted in a passive margin is 0.75 psi/ft) is consistent with a maximum stress horizontal (i.e. parallel to the thrust direction) and not vertical as in most passive basins. The maximum horizontal stress is quite difficult to estimate. Using rock strenght measured on core and breakouts initiation σ_H was found to lie between 1.2psi/ft and 1.5 psi/ft.

Stress rotations in the vicinity of faults

The D.S.C.A. method proposed in the mid-seventies by Simmons et al[22,23] relates the current in situ stress state with the microcrack network induded when the rock is relaxed (by coring for instance) from the pre-existing stress state. Experimentally, the method consits of cutting a cubic-shaped sample from the microcracked relaxed core then fitting with strain gauges. After moulding in a rubber envelope, the specimen is loaded hydrostatically in a pressure vessel. Under increasing confining pressure the microcracking information corresponds to the non linear part of the stress strain curve.
Two series of ten tests have been carried out on cores issued from the Mirador (reservoir) of two different wells. As pointed out on **Fig. 2**, for well 1 the major stress is pseudo horizontal whereas for well 2, which is closer to the Cusiana fault, the major stress is nearly vertical. In spite of a general tectonic direction parallel to the thrust, in the vicinity of major faults, stress rotations can be observed. This point will be studied in more detail in the next paragraph devoted to field scale modelling.

Foothills scale modelling : stress state induced by the Cusiana fault

To better understand the role of faults, finite element simulations were performed with GEOSIM2D[24,25]. This code allows performing 2D large strain simulations.

To simplify, only the Cusiana thrust fault was considered and erosion and sedimentation processes were not integrated in the simulations. The whole structure (**Fig. 7**) is made of a deformable hangingwall (Cusiana block) displacing relatively to a footwall (basement and Llanos block). At the beginning of the simulations, the weight is set. Then, the tectonic compression is simulated by applying a uniform horizontal displacement at the left boundary of the hangingwall block. On both vertical sides of the basement/Llanos block roller boundary conditions are considered. The bottom of the model is fixed while the top surface is free. The fault is modelled by a listric frictional interface (Coulomb friction law).

The main goal was to record the stress state in the Cusiana block versus the tectonic push for different shortening values then to compare these results with available field values.

A first set of simulations were performed considering an elastic rheology and an unlocked fault (zero friction coefficient). If the Young's modulus of the hangingwall is relatively high (5000 MPa), it is not possible to accommodate with the geometry of the Cusiana fault. Consequently, void opening occurs where the curvature is maximum (**Fig. 8a**). The strong bending moment imposed at the base of the hangingwall generates an horizontal tensile stress at great depth (**Fig. 8b**). This result is not physically acceptable regarding the in situ stresses which increase with depth and always remain compressive.

To obtain a more realistic stress gradient and to prevent void opening, it is necessary to decrease the stiffness of the Cusiana block. With a Young's modulus five times smaller (E=1000MPa) void opening disappears and the horizontal stress increases monotonously with depth (**Fig. 9**). Nevertheless, the bending effect is still obvious since for the last time step the horizontal stress gradient decreases. Furthermore, the horizontal stress reaches unrealistic values at the surface for the last time steps (more than to 120 MPa for 3200m shortening). This result is attributed to the absence of plastic threshold.

In a second set of simulations, the footwall/basement structure remains elastic whereas the hangingwall is modelled by an ideal elastoplastic Von Mises yield criterion (the only plastic parameter required is the cohesion - it is taken equal to 5 MPa) whereas the fault remains unlocked (zero friction coefficient). The introduction of such a plastic limit allows the horizontal stress to drop at surface where it only exceeds 10 MPa for the last shortening step (**Fig. 10a**). Versus depth, the horizontal stress gradient ranges between 1.2psi/ft to 1.4psi/ft, a value which agrees with the field data.

The kinematical evolution of the structure as shortening progresses is visualized by mapping the isocontours of the equivalent plastic strain (also called distortion) which is a scalar proportional to the second invariant of the strain deviator that is

$$\gamma^p = \sqrt{\frac{2}{3}\left[\left(\varepsilon_1^p - \varepsilon_2^p\right)^2 + \left(\varepsilon_1^p - \varepsilon_3^p\right)^2 + \left(\varepsilon_2^p - \varepsilon_3^p\right)^2\right]}$$

where $\varepsilon_1^p, \varepsilon_2^p, \varepsilon_3^p$ are the principal plastic strain components. The distortion isocontours show where large plastic strains localize (**Fig. 11**). As shortening progresses, plastic distortion initially (i.e. after setting the weight) homogeneous at a given depth quickly concentrates at the

base of the hangingwall where the curvature of the Cusiana fault is maximum. This localization which develops inside a shear band moving towards the surface clearly corresponds to the backthrust observed on the seismic section of **Fig. 3**. The second localization zone initiating at the left bottom wedge of the hangingwall results from a local effect and has not a real physical meaning.

The tectonic push also induces large stress rotations. Just after setting the weight, the minor principal stress is horizontal. As the Cusiana block deforms, the stresses quickly rotate of a 90° angle in the major part of the hangingwall except in the vicinity of the Cusiana fault where the vertical stress remains maximum. This is illustrated on **Fig. 12** where the angle between the major stress and the vertical (0° corresponds to a vertical major stress) is plotted along an horizontal cross section at the top reservoir. At the end of the simulation (maximum shortening), the major stress which is horizontal over a distance of 17 km sharply rotates and becomes pseudo-vertical next to the Cusiana fault. This wedge-induced stress rotation is consistent with the set of DSCA tests performed on core samples from the Mirador formation on wells 1 and 2 (**Fig. 3**).

If a friction coefficient along the thrust fault is introduced the results significantly change. First of all, it is not possible to use a Von Mises criterion since the internal friction angle of the material (equal to zero in the case of a Von Mises) has to be higher than the friction angle of the fault. Otherwise, a high stress concentration appears at the very beginning of the simulation in the element located at the left bottom wedge of the hangingwall. This induces locally a very large plastic strain which makes the calculation diverge. Consequently, the material has to be modelled by using a Drucker-Prager elastoplastic constitutive law. This introduces an extra parameter (friction angle of the material).

As shown in **Fig. 13** and contrarily to the previous case, instead of developing a backthrust, the equivalent plastic strain localises near the surface in a zone roughly homothetic to the Cusiana fault. The horizontal stress profile along a vertical cross section shows three different stress regimes: a gradient higher than 3 psi/ft and corresponding to the plastic domain at shallow depth, a decreasing gradient in the intermediate elastic zone where bending occurs and a second overcompressive zone when approaching the fault. This domain remains elastic due to the conjugated effect of high confining pressure and material friction angle. The computed stress values clearly overestimate the stress gradient which is higher than 2 psi/ft.

To sum up, only simulation 3 leads to coherent results both from kinematical (localisation of the plastic strain along a backthrust) and mechanical (reasonable values of the horizontal stress gradient) viewpoints.

Conclusion

The finite element simulations presented in this paper combine large strain and discontinuities capabilities to model the mechanical behaviour of geological structures. Currently only 2D plane strain modeling has been performed.

In the foothills region, systematic measurements of borehole breakouts remarkably confirm the NW-SE trend but, presence major faults can cause major rotations.

The geological setting of the Cusiana anticline has been simulated from an initial unstrained geometry. Only the Cusiana fault was taken into account. The main results can be summarized as follows. When adressing to a geological structure, the very low strain rates are not compatible with constitutive laws calibrated on laboratory core samples. To reproduce reasonable kinematical scenarii and coherent stress gradients, it is necessary to use soft materials sliding on low frictional interfaces. With a too high Young's modulus the hangingwall is not able to accommodate the curvature of the Cusiana fault which induces tractions at great depth. Moreover, even if one considers a low friction coefficient (i.e. 8°) along the fault, the computed stress gradients are abnormally high (more than 2psi/ft) and plasticity which only concentrates at the surface does not generate the backthrust observed on the geological section. On the opposite, the use of a perfectly sliding thrust fault is compatible with the observed antithetic fault.

This result is nothing other than the expression of the viscosity (both for material and interface) which is dominant when deforming at very low strain rates (in the range of 10^{-14}/s). In other words, elastoplastic rheologies with weak mechanical properties (i.e. Young's modulus and plastic cohesion) make it possible to reproduce complex viscous behaviours over large time and length scales.

Besides structural geology, such numerical modelling can be applied to various practical petroleum applications e.g. fluid migration in sedimentary basins, drilling optimization in highly tectonic areas, detection of abnormal pore pressures, better characterization of fractured reservoirs... In this scope, the use of more complex constitutive laws including damage and anisotropy[26] and the implementation of fluid flow are of prime importance. For the future, the latter should be a main issue in so far it will require generalization of poromechanics theory to finite strains[27,28].

Aknowlegements

The authors thank TEPMA Colombie, BP exploration, Triton and Ecopetrol for allowing to publish this paper.

References

1.Cazier, E. C., A. B. Hayward, G. Espinosa, J. Velandia, J. F. Mugniot, and W. G. Leel (1995) "Petroleum geology of the Cusiana field, Llanos basin foothills" Colombia, Am. Assoc. Pet. Geol. Bull., 79, 10, 1444-1463.

2. Last, N., R. Plumb, R. Harkness, P. Charlez, J. Alsen, M. McLean (1995) "An integrated approach to evaluating and managing wellbore instability in the Cusiana field, Colombia, South America", paper presented at the Seventieth Annual Technical Conference & Exhibition, Soc. of Pet. Engin., Dallas, October 22-25. SPE 30464

3. Haimson B. and Ch. Fairhurst (1969) "In situ stress determination at great depth by means of hydraulic fracturing" 11th Symposium on Rock Mechanics. Berkeley pp 559-584

4. Cox J.W. (1970) "The high resolution dipmeter reveals dip-related borehole and formation characteristics" Prof. Well Log Analysts.

5. Charlez, P. A., C. Hamamdjian and D. Despax (1986) "Is the microcracking of a rock a memory its initial state of stress?" International Symposium on Rock Stress, Stockholm, September 1-3,1986.

6. Engelder, T. (1993) "Stress regimes in the lithosphere", 457 pp., Princeton University Press, N. J

7. Hafner, W (1951) "Stress distibutions and faulting", Geol. Soc. of Am. Bull., 62, 373-398.

8. Sanford, A.R. (1959) "Analytical and experimental study of simple geologic structures", Geol. Soc. of Am. Bull., 70, 19-52.

9. Wdowinski, S., and R. J. O'Connell, "Deformation of the central Andes (15°, 27°S) derived from a flow model of subduction zones", J. Geophys. Res., 96, 12245-12255, 1991.

10. Whittaker, A., M. H. P. Bott and G. D. Waghorn, "Stresses and plate boundary forces associated with subduction plate margins", J. Geophys. Res., 97, 11933-11944, 1992.

11. Zhong, S., and M. Gurnis (1994) "Controls on trench topography from dynamic models of subducted slabs", J. Geophys. Res., 99, 15683-15695

12. Baumont, C., P. Fullsack, and J. Hamilton (1994) "Styles of crustal deformation in compressional orogens caused by subduction of the underlying lithosphere", Tectonophysics, 232, 119-132

13. Bott, M. H. P. (1993) "Modelling the plate-driving mechanism", J. Geol. Soc. London, 150, 941-951.

14. Tharp, T. M.(1985), "Numerical models of subduction and forearc deformation", Geophys. J. R. Astron. Soc., 80, 419-437.

15. Maekel, G., and J. Walters (1993) Finite-element analyses of thrust tectonics: computer simulation of detachment phase and development of thrust faults, Tectonophysics, 226, 167-185

16. Nieuwland, D. A. and J. V. Walters (1993) Geomechanics of the south furious field. An integrated approach towards solving complex structural geological problems, including analogue and finite-element modelling. Tectonophysics, 226, 143-166, 1993.

17. Cooper, M.A., F.T. Addison, R. Alvarez, M. Coral, R.H. Graham, A.B. Hayward, S. Howe, J. Martinez, J. Naar, R. Penas, A.J. Pulham, and A. Taborda (1995) "Basin development and tectonic history of the Eastern Cordillera and Llanos basin, Colombia" Am. Assoc. Pet. Geol. Bull., 79, 10, 1421-1443

18. Casero, P., R. Afrasmanech, L. Martin, D. Michoux, C. Osorio, J. F. Salel, A. Rossato, J. J. Aristizabal, C. Lombo, P. A. Rios, and M. Nowak (1995) Stuctural evolution of the margin and foothills belt of the Cordillera Oriental of Colombia (southwest of Colombia), paper presented at the Sixth Colombian Petroleum Congress, Santafe de Bogota, December 3-6.

19. Bell, J. S. and D. I. Gough (1979) North East-South West compressive stress in Alberta: evidence from oil wells, Earth Planet. Sci. Lett., 45, 475-482.

20. Guenot, A. (1987) Contraintes et ruptures autour des forages pétroliers, in Proceedings of the Sixth International Congress on Rock Mechanics, pp. 109-118, Balkema, Rotterdam.

21 Haimson B. C. and I. Song (1993) Laboratory study of borehole breakouts in Cordova Cream: a case of shear failure (abstract), Int. Jour. Rock Mech. Min. Sc & Geomech., 30(7), 1047-1056.

22. Simmons, G., R. W. Siegfried and M. Feves (1974) Differential strain analysis: a new method for examining cracks in rocks, J. Geophys. Res., 79, 4383-4385, 1974.

23. Hamamdjian, C., (1989) "Détermination de l'état de contrainte géostatique par l'étude de la microfissuration des roches", Ph. D., 193 pp., Ecole Centrale de Paris, 1989.

24. Bathellier, E., Calculs des localisations de déformations tectoniques avec éléments finis, Ph.D. thesis, 324 pp., Ecole Centrale de Paris, 1994.

25. Plischke, B., R. Dallmann, and J. F. Chedmail (1991) "Numerical simulations of geological processes, in Proceedings of the Seventh International Congress on Rock Mechanics, pp. 1909-1912, Balkema, Rotterdam".

26. Dragon A., Ph. Charlez, D. Pham and J. F. Shao, A model of anisotropic damage by (micro)crack growth, in Assessment and Prevention of failure Phenomena in Rock Engineering, pp. 71-78, Balkema, Rotterdam, 1993.

27. Coussy, O., Mécanique des milieux poreux, 464 pp., Technip, Paris, 1991.

28. Bourgeois, E., P. de Buhan and L. Dormieux, Formulation d'une loi élastoplastique pour un milieu poreux saturé en transformation finie, C. R. Acad. Sci. Paris, 321, 175-182, 1995.

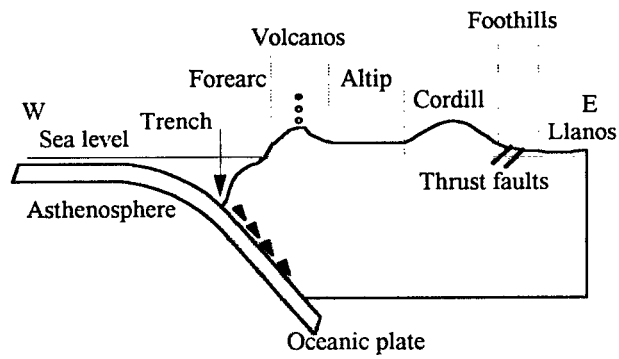

Fig. 1 - Stress regimes in the Andin Cordillera (*adapted from Wdowinski and O'Connell, 1991*)

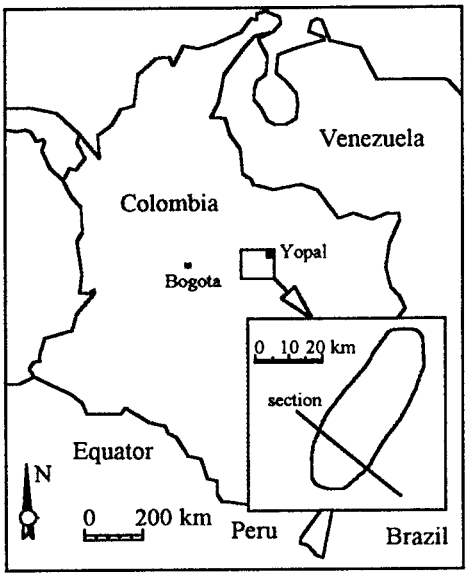

Fig. 2 - Location of the Cusiana field

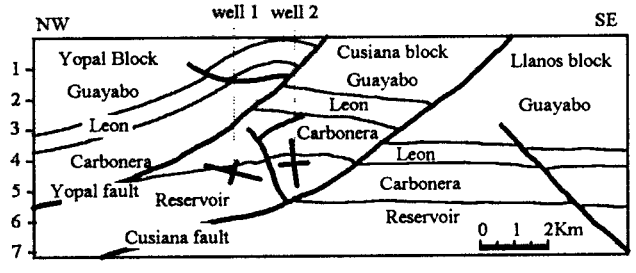

Fig. 3 - NW-SE geological cross section of the Cusiana field

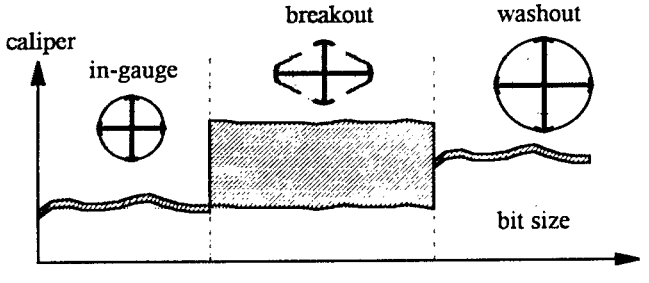

Fig. 4 - Breakout, washout and in gauge sections

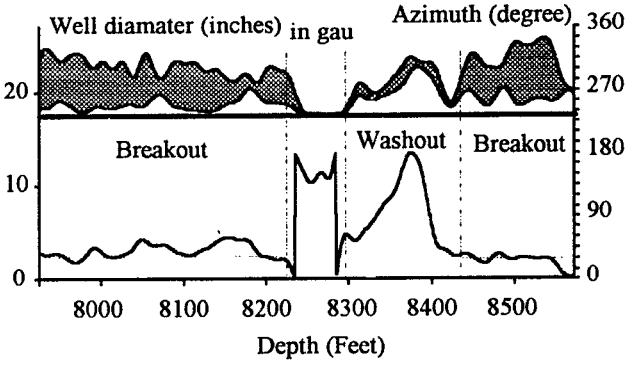

Fig. 5 - Actual calliper section of a Cusiana well

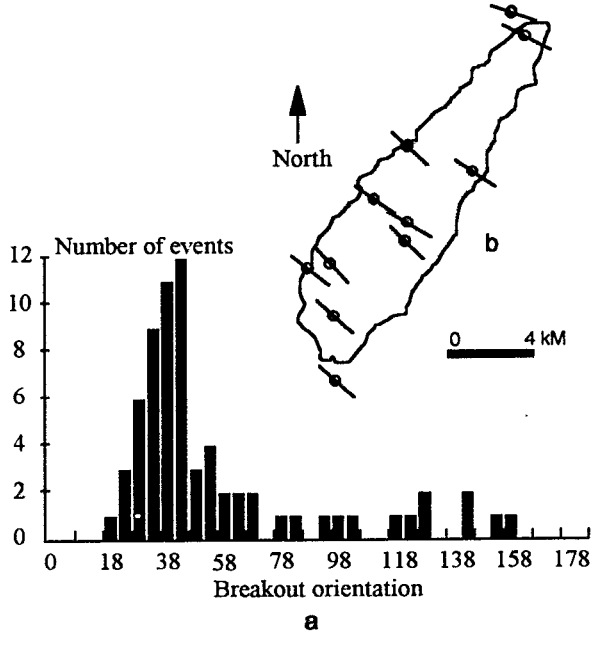

Fig. 6 - General results of breakout analysis
a - Distribution of events over 8 wells
b - Orientation of average major stress

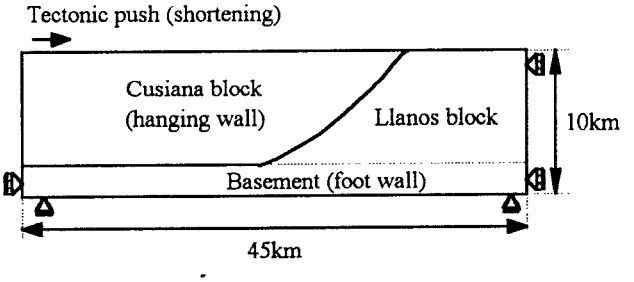

Fig. 7 - Hanging wall/footwall model

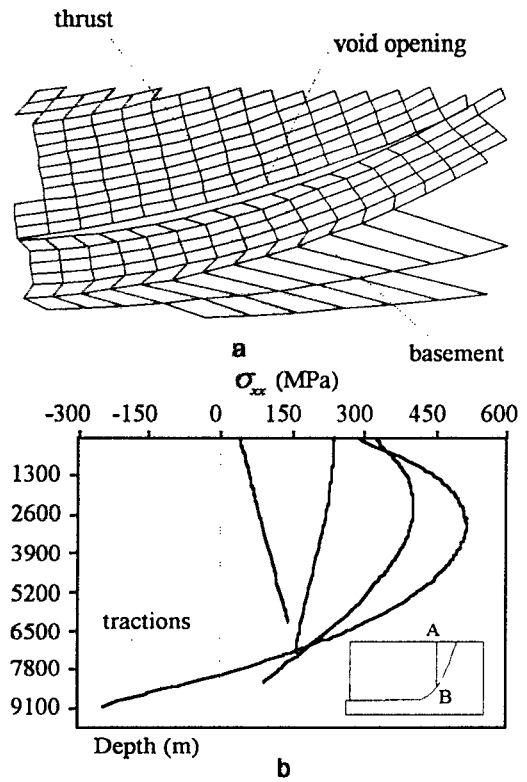

Fig 8 - Elastic calculation (5000 MPa Young's modulus)
a - Enlargement of the finite element mesh.
b. Horizontal stress profile along the vertical section AB.

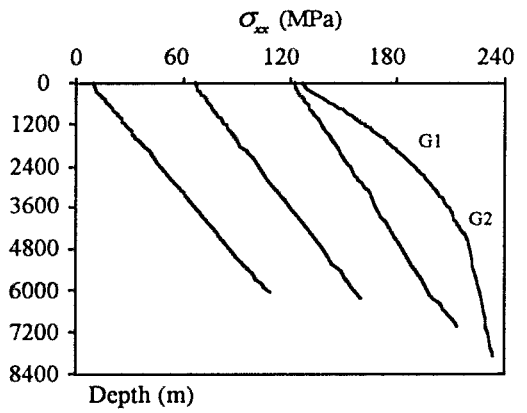

Fig. 9 - Horizontal stress profiles at different time steps (E=1000 MPa) (cross section AB)

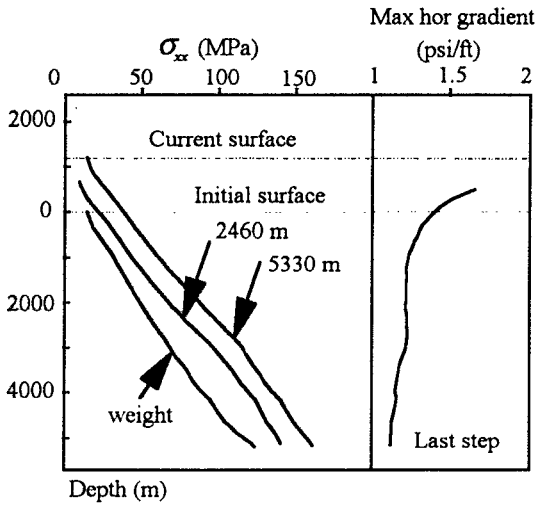

Fig. 10 Von Mises model - Non frictionnal fault

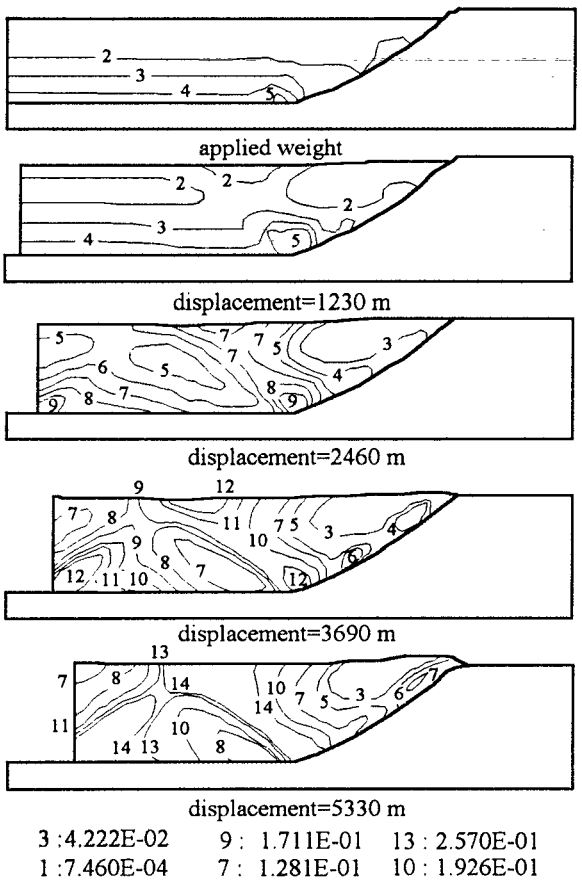

Fig 11 - Isocontours of equivalent plastic strain showing the initialization of a *"pop-up"*.

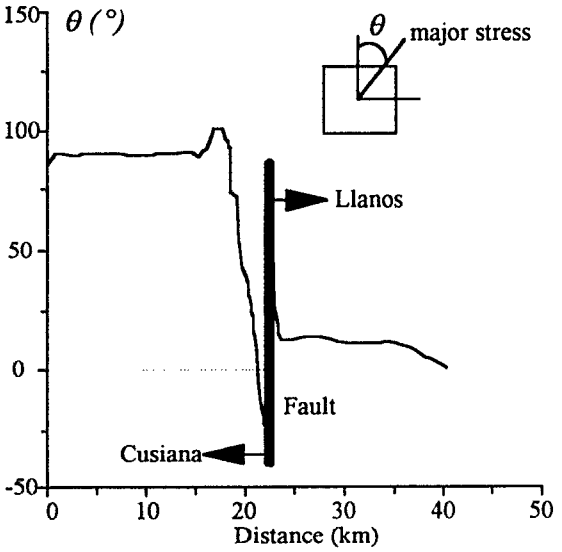

Fig. 12 Stress rotation when approaching the Cusiana fault (Mises material and zero sliding fault).

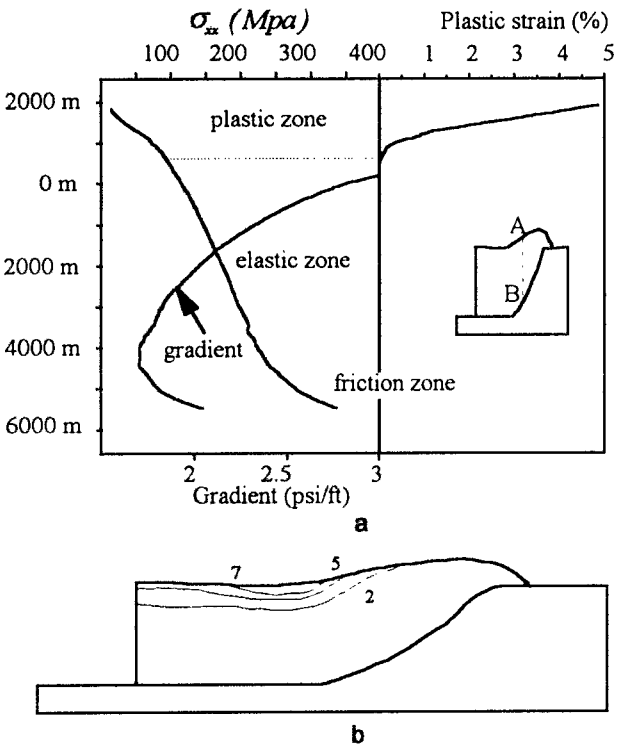

Fig. 13 - Horizontal stress profile and associated gradient for a Drucker-Prager material and a frictional fault (a) Isocontours of equivalent plastic strain (b)